International Journal of Nanoelectronics and Materials
IJNeaM
ISSN 1985-5761 | E-ISSN 2232-1535

Influence of infill pattern on tensile strength and material efficiency of fused deposition modelling (FDM)-printed polylactic acid (PLA) parts

Md Ashequl Islam [a,b], Khairul Salleh Basaruddin [a,b] *, Mahbub Hassan [c], Nur Saifullah Kamarrudin [a], Azrin Hani Abdul Rashid [d], and Tien-Dat Hoang [e]

[a]*Faculty of Mechanical Engineering & Technology, Universiti Malaysia Perlis, Arau, Malaysia, Arau 02600, Malaysia*
[b]*Motorsports Technology Centre of Excellence, Universiti Malaysia Perlis, Arau, Malaysia, Arau 02600, Malaysia*
[c]*Faculty of Civil Engineering & Technology, Universiti Malaysia Perlis, Arau, Malaysia, Arau 02600, Malaysia*
[d]*Faculty of Engineering Technology, Universiti Tun Hussein Onn Malaysia, Pagoh Campus, 84600 Pagoh, Johor, Malaysia*
[e]*School of Mechanical and Automotive Engineering (SMAE), Ha Noi University of Industry, Vietnam*
** Corresponding author. Tel.: +60139278004; e-mail: khsalleh@unimap.edu.my*

Received 12 September 2025, Revised 1 October 2025, Accepted 10 October 2025

ABSTRACT

This study investigates the influence of infill patterns and densities on the tensile properties of Fused Deposition Modeling (FDM) 3D-printed Polylactic Acid (PLA) parts, aiming to optimize material efficiency while maintaining structural integrity. Eight infill patterns—Cross 3D, Subdivision Cubic, Octets, Quarter Cubic, Concentric, Grid, Gyroid, and Zigzag—were tested at 45%, 55%, and 65% infill densities, with a solid specimen (100% infill) serving as a benchmark. Tensile testing revealed that the Quarter Cubic pattern at 65% infill density closely matched the mechanical strength and stiffness of the solid specimen while significantly reducing material usage. Statistical analysis using the Taguchi method and ANOVA identified infill percentage as the most influential factor ($p = 0.003$), while regression modeling ($R^2 = 91.88\%$) demonstrated robust predictive capability. This study contributes novel insights into the interplay between infill design and mechanical performance, guiding sustainable production of high-strength, lightweight PLA components for applications in aerospace, automotive, and consumer products.

Keywords: *Additive manufacturing, Polylactic acid, Tensile strength, Fused deposition modeling (FDM), Process optimization, Taguchi method*

1. INTRODUCTION

Additive manufacturing (AM), particularly Fused Deposition Modeling (FDM), has become a cornerstone of Industry 4.0 due to its versatility, customization potential, and sustainable manufacturing practices. The expiry of foundational FDM patents in 2010 catalyzed widespread adoption, especially for applications requiring rapid prototyping and complex geometries [1–5]. PLA, a biodegradable polymer derived from renewable resources, is among the most commonly used FDM materials due to its ease of processing, dimensional stability, and environmental benefits [6–8].

Despite these advantages, the mechanical properties of FDM-printed PLA parts, particularly tensile strength and stiffness, often underperform compared to conventionally manufactured counterparts. This discrepancy is largely due to interlayer adhesion limitations and process parameter sensitivity [9–11]. Previous research has examined individual parameters such as print speed, temperature, and layer thickness, with some studies also evaluating infill density or pattern [12–14]. However, limited work has holistically analyzed their combined effects using rigorous statistical tools.

Polylactic Acid (PLA), a biodegradable polymer derived from renewable sources, is among the most commonly used materials in FDM. It is prized for its biocompatibility, dimensional stability, low toxicity, and moderate mechanical strength [6, 12]. However, despite these advantages, the mechanical performance of FDM-printed parts, particularly their tensile strength and elastic modulus, often lags behind those produced by conventional means, primarily due to interlayer adhesion issues and parameter sensitivity [13–15].

Previous studies have explored how FDM process parameters, such as layer thickness, build orientation, infill density, pattern geometry, and extrusion temperature, influence the mechanical behavior of PLA specimens. For instance, Patel *et al.* [16] showed that specimens built in the on-edge orientation with higher infill density exhibited superior tensile performance. Chacón *et al.* [17] demonstrated the role of feed rate and layer thickness in optimizing tensile and flexural properties, while Alafaghani *et al.* [18] employed the Taguchi method to determine optimal conditions for strength and dimensional precision, highlighting the significance of triangular infill at high density and moderate temperatures.

The COVID-19 pandemic further underscored the strategic importance of FDM/FFF, as it was rapidly deployed for local, on-demand production of critical items such as face shields, nasal swabs, and ventilator components [19–21]. Yet, despite iremainen utility, the mechanical reliability of printed parts remains a primary concern, particularly in load-bearing or high-performance applications.

Recent investigations have recognized that combinations of process parameters, rather than individual ones, significantly influence final part quality. However, limited research has addressed the synergistic effects of infill geometry and density, two parameters known to impact porosity, stress distribution, and fracture behavior [22–24]. Moreover, complex interdependencies among these variables create challenges in predicting and optimizing mechanical performance [25–27].

This study presents a comprehensive and statistically rigorous investigation into the combined effects of infill pattern geometry and density on the tensile performance of FDM 3D-printed PLA parts—an area that has been previously underexplored in a holistic manner. Unlike earlier research that evaluated these parameters in isolation, this work applies the Taguchi method and ANOVA to identify the dominant influence of infill density and uses regression modeling to develop a predictive framework for tensile strength optimization. We aim to identify optimal combinations that balance material use with structural integrity, providing actionable strategies for high-performance, sustainable FDM fabrication.

2. MATERIALS AND METHODS

2.1. Materials and Methods

Polylactic Acid (PLA), a biodegradable thermoplastic polymer derived from renewable resources such as corn starch or sugarcane, was selected as the printing material for this study due to its favorable mechanical properties, low cost, and environmental sustainability. PLA has become one of the most extensively used materials in fused deposition modeling (FDM)-based 3D printing, owing to its ease of processing, dimensional stability, and non-toxic nature. Its mechanical performance, comprising a good balance of tensile strength, stiffness, and impact resistance, makes it well-suited for applications ranging from rapid prototyping and biomedical devices to packaging and lightweight structural components [29–31].

Compared to many petrochemical-based polymers, PLA offers comparable strength and rigidity while being more environmentally friendly due to its biodegradability and lower carbon footprint [32, 33]. These attributes have led to their increased use in sustainable manufacturing and circular economic initiatives, especially in additive manufacturing environments where material efficiency is critical.

In this study, the PLA filament used had a diameter of 1.75 mm, a purity exceeding 98%, a density of 1.24 g/cm^3, and a melting temperature of 160°C, consistent with industrial-grade specifications. To ensure consistency and high print quality, the filaments were pre-dried in a vacuum oven at 60°C to minimize moisture absorption. PLA is hygroscopic, and moisture uptake can lead to hydrolytic degradation during extrusion, resulting in inferior layer adhesion, surface roughness, and the emission of fumes during printing [34, 35]. Pre-drying is thus the best standard practice to preserve material integrity and optimize the mechanical performance of printed specimens.

2.2. Specimen Design and Printing Process

The specimen design in this study adhered to the ASTM D638 Type IV standard, which is widely recognized for the tensile testing of plastic materials. This standard specifies the use of a dog-bone-shaped geometry, chosen for its effectiveness in promoting uniform stress distribution along the gauge length during mechanical testing [35]. As illustrated in Figure 1, the specimens were designed using computer-aided design (CAD) software and exported as STL files for slicing. The slicing process was conducted using specialized software that enabled customization of critical printing parameters to meet the specific experimental requirements.

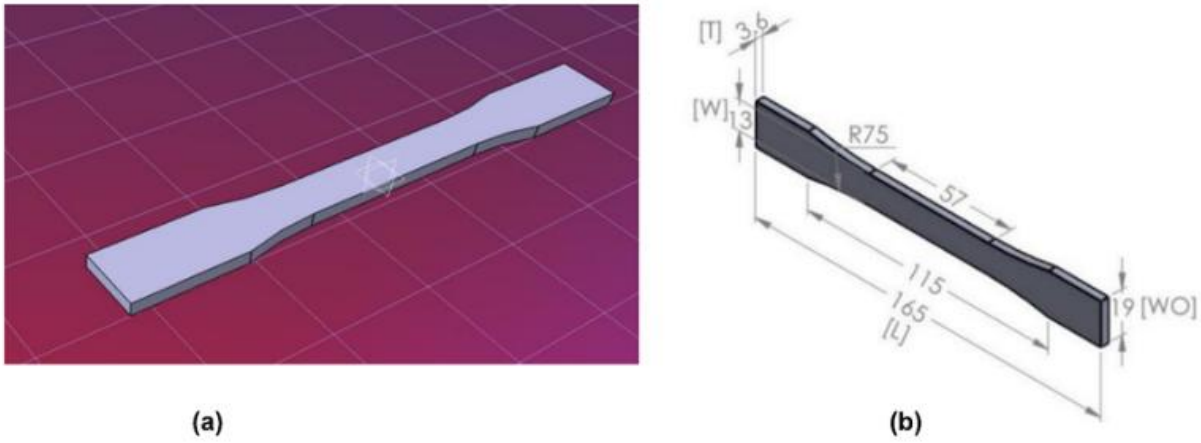

Figure 1. (a) 3D model for the dog bone-shaped specimen and (b) dimensions of the impact test sample according to ASTM D638

The influence of internal structure on mechanical performance, eight distinct infill patterns, including Cross 3D, Subdivision Cubic, Octets, Quarter Cubic, Concentric, Grid, Gyroid, and Zigzag, were selected for this study. These patterns provide a variety of internal geometries, each offering different degrees of stiffness, strength, and material efficiency, as depicted in Figure 2. Each infill pattern was tested at three density levels: 45%, 55%, and 65%, with a 100% solid infill specimen included as a benchmark for comparative analysis. These densities were selected to explore the trade-off between material usage and mechanical performance, where lower densities were anticipated to reduce PLA consumption and print time but potentially result in lower tensile strength due to increased internal porosity [36–38].

The specimens were fabricated using an Ender 5 Pro 3D printer, as shown in Figure 3, a widely adopted FDM/FFF system developed by Shenzhen Creality 3D Technology Co., Ltd. This printer was chosen for its high reliability, consistent print quality, and resumption capability after power failures. With a build volume of 220 × 220 × 300 mm, the Ender 5 Pro provided the dimensional capacity and accuracy necessary for consistent fabrication across all test specimens [39, 40].

Key process parameters, including nozzle temperature, bed temperature, layer height, and print speed were carefully controlled, as detailed in Table 1, to minimize variability and ensure consistent part quality. The layer height was set below the nozzle diameter to enhance

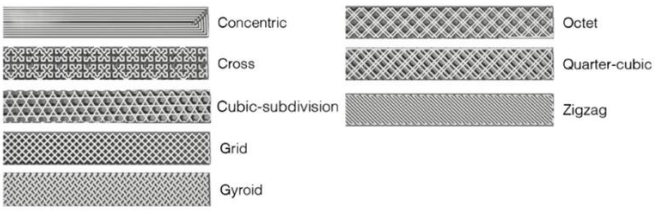

Figure 2. Design of unique infill patterns and different infill densities

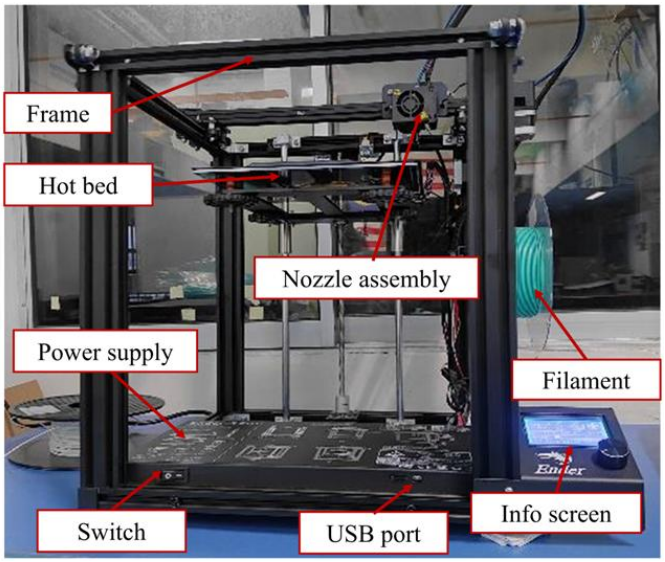

Figure 3. FDM 3D printer setup for printing specimens

Table 1. Process parameters for 3D printing

Parameters	Set values
Printing temperature (°C)	200–220
Printer bed temperature (°C)	60
Printing speed (mm/s)	30–50
Nozzle flow (%)	100
Build plate adhesion type	None
Height of layer (mm)	0.2
Thickness (mm)	5.0
Diameter of Nozzle (mm)	0.4
Raster angle	0° alignment with the printing axis

interlayer bonding and reduce intra-layer porosity, which is critical for achieving reliable mechanical performance in FDM-printed parts [41]. A raster angle of 0° was selected so that the printed filament paths aligned with the direction of tensile loading, thereby optimizing the load-bearing capacity of the specimens during tensile testing [42, 43].

2.3. Tensile Testing

The tensile properties of each 3D-printed specimen were evaluated using a Universal Testing Machine (UTM) with a maximum load capacity of 250 kN, as depicted in Figure 4(a). Testing was conducted in accordance with the ASTM D638 standard for tensile characterization of plastic materials [44]. Each specimen was subjected to uniaxial tensile loading until failure, as illustrated in Figure 4(b). During testing, specimens were securely clamped in the machine grips, ensuring precise alignment of the gauge length with the direction of the applied load to prevent bending or torsional effects.

Real-time acquisition of load and displacement data was carried out throughout the test to generate detailed engineering stress-strain curves. From the initial linear portion of each curve, Young's Modulus was calculated, reflecting the material's elastic stiffness. The Ultimate

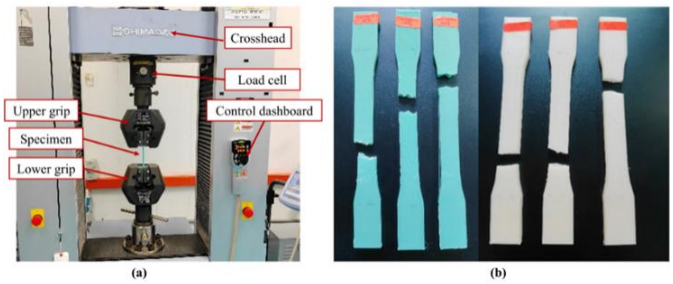

Figure 4. (a) Tensile testing setup using a Shimadzu Universal Testing Machine (b) Fractured 3D-printed PLA specimens after tensile testing

Tensile Strength (UTS) was identified as the peak stress reached prior to specimen failure, providing a direct measure of tensile load-bearing capacity [45, 46].

Post-fracture analysis of the specimens was conducted to examine failure modes and identify potential defects such as poor interlayer adhesion, void formation, and raster orientation mismatch, all of which can significantly influence tensile performance in FDM-printed parts [47–49]. Particular attention was paid to the variation in fracture surface morphology across different infill patterns and densities, as these structural characteristics directly affect stress distribution, energy absorption, and crack propagation paths within the printed material [50, 51].

Insights from this fractographic evaluation were used to draw conclusions on the mechanical reliability and design optimization potential of various infill configurations for applications requiring lightweight yet durable polymer components. Such analysis is critical for informing real-world design strategies in sectors such as biomedical devices, automotive, and aerospace, where material efficiency and mechanical integrity must be balanced [52, 53].

2.4. Design of Experiment (DOE)

Understanding how Fused Deposition Modeling (FDM) process parameters influence the mechanical properties of printed parts is essential for improving the performance, reliability, and applicability of additively manufactured components [54]. In this investigation, a Design of Experiments (DOE) approach using the Taguchi method was adopted to identify the optimal combination of parameters for maximizing the Ultimate Tensile Strength (UTS) of PLA specimens fabricated via FDM. An L9 orthogonal array (Taguchi L9(3^4)) was generated using Minitab 2021 software to systematically vary four key process parameters: infill pattern, infill percentage, print speed, and extrusion temperature, each at three levels, as detailed in Table 2.

The Taguchi method was chosen for its efficiency in reducing the number of experimental runs while maintaining the ability to detect the most influential factors with statistical rigor. This structured approach minimizes testing time and cost without compromising the quality of conclusions [55, 56]. Table 3 outlines the selected parameter combinations and the corresponding number of experimental trials. Each parameter set was replicated across three identical specimens, resulting in a total of 27 tensile tests. This replication ensured data reliability and minimized the effects of random experimental errors, enhancing the repeatability and statistical validity of the results.

The significance of each parameter's influence on UTS was determined using a one-way Analysis of Variance (ANOVA). ANOVA provided insight into the degree to which each factor contributes to the observed variability in the mechanical responses. Furthermore, the signal-to-noise (S/N) ratio was employed as a Taguchi optimization metric to determine the robustness of parameter settings against external noise and variability. In this study, all mechanical property outcomes were considered "larger-is-better" quality attributes. Accordingly, Equation (1) was used to calculate the S/N ratio for each experimental run:

$$S/N = -10 \log\left(\frac{1}{n}\sum_{i=1}^{n}\frac{1}{y^2{}_i}\right) \quad (1)$$

where S/N is the signal-to-noise ratio, y_1, y_2, y_3 are the output responses UTS from replicated tests, and n is the number of replications ($n = 3$ in this case).

This Taguchi-based experimental strategy provides a statistically sound and resource-efficient method for identifying optimal printing parameters in FDM-printed PLA parts, contributing to the growing body of knowledge aimed at enhancing the functional performance and sustainability of 3D-printed materials.

Table 2. Process parameters and their ranges

Name of parameters	Levels		
	1	**2**	**3**
Infill pattern	Subdivision Cubic	Quarter Cubic	Zig Zag
Infill percentage (%)	45	55	65
Print speed (mm/sec)	30	40	50
Extrusion temp (℃)	200	210	220

Table 3. Taguchi L9 (34) orthogonal array

Run	Infill pattern	Infill percentage (%)	Print speed (mm/sec)	Extrusion temp (℃)
1	1	45	30	200
2	1	55	40	210
3	1	65	50	220
4	2	45	40	220
5	2	55	50	200
6	2	65	30	210
7	3	45	50	210
8	3	55	30	220
9	3	65	40	200

3. RESULTS AND DISCUSSION

The mechanical performance of 3D-printed PLA components is significantly influenced by infill density and pattern selection. In this study, specimens printed with a 65% infill density demonstrated notably higher tensile strength compared to those with 45% and 55% densities, as depicted in Figure 5. This enhancement is primarily attributed to reduced void spaces and improved interlayer bonding at higher densities, leading to superior load-bearing capacity and stiffness. These findings align with previous research indicating that increased infill density enhances tensile strength due to better structural integrity and material continuity [17–20].

Among the eight infill patterns evaluated, Subdivision Cubic, Quarter Cubic, and Zigzag consistently outperformed others across all infill densities. Its geometric configuration facilitates uniform stress distribution, contributing to higher strength and stiffness. Conversely, patterns like Cross 3D, Grid, and Gyroid exhibited lower tensile strength, potentially due to less efficient load distribution inherent in their structures.

Figure 6 illustrates the force-displacement curves for specimens with varying infill patterns and densities. The "Solid" infill pattern achieved the highest force capacity and ultimate displacement, underscoring its superior mechanical strength and ductility. Patterns such as "Cubic Subdivision Octet," "Quarter Cubic," and "Zigzag" displayed moderate performance, balancing strength and deformation capacity. In contrast, "Cross 3D" and "Grid" patterns showed lower force capacities and earlier failure, especially at lower densities, likely due to their less robust internal structures.

As infill density increased from 45% to 65%, a corresponding rise in peak force was observed across all patterns, indicating enhanced load-bearing capacity. However, the displacement at failure remained relatively consistent for each pattern, suggesting that while density influences strength, it has a limited effect on the material's flexibility. These trends corroborate findings from recent studies emphasizing the critical role of infill density and pattern in determining the mechanical properties of 3D-printed PLA parts [33, 34].

Figure 7 illustrates the ultimate tensile strength (UTS) data of FDM 3D-printed PLA specimens, assessed for normality using a normal probability plot. In this plot, blue points

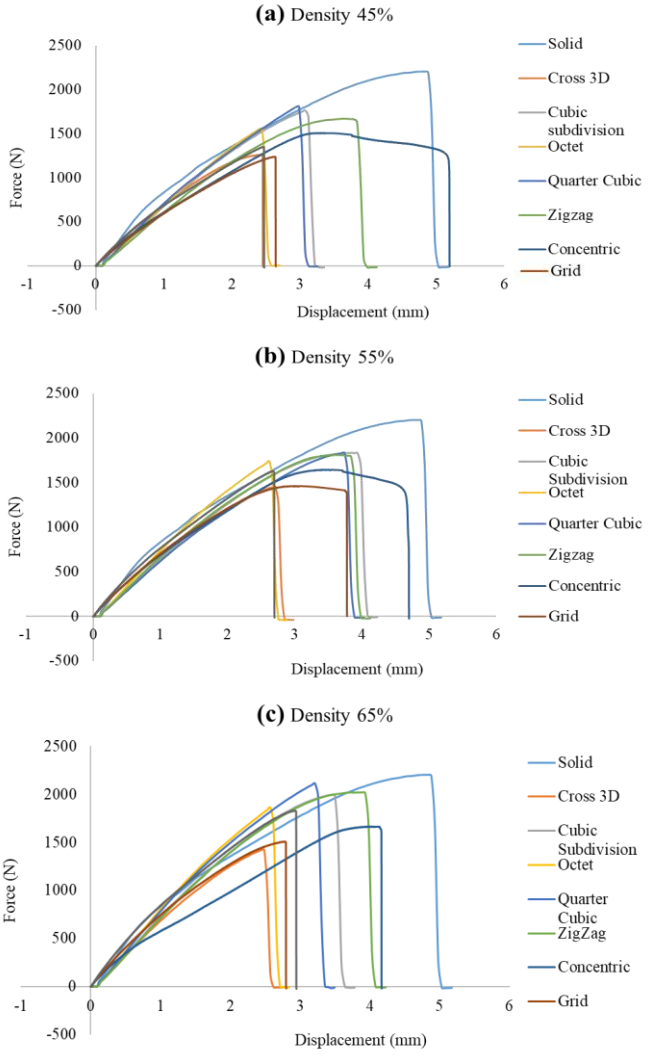

Figure 6. Force vs. displacement curves for PLA specimens printed with different infill patterns at (a) 45%, (b) 55%, and (c) 65% infill densities.

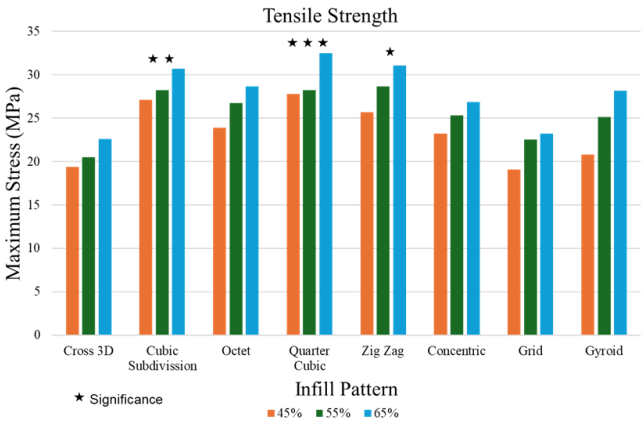

Figure 5. Comparison of the tensile strength for all infill densities and patterns

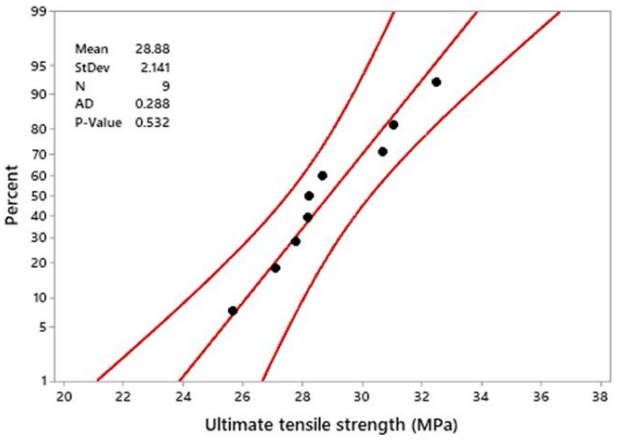

Figure 7. Normal probability plot of ultimate tensile strength

represent the observed data, the central red line indicates the fitted normal distribution, and the outer red lines denote the 95% confidence intervals. The alignment of data points along the central line suggests conformity to a normal distribution.

Anderson–Darling (AD) normality test was applied to statistically confirm this observation. The AD test evaluates whether a dataset follows a specified distribution, with the null hypothesis stating that the data are normally distributed. A p-value greater than 0.05 indicates no significant deviation from normality. In this case, the p-value obtained was 0.532, exceeding the 0.05 threshold, thereby supporting the null hypothesis and confirming the normality of the UTS data.

The normal probability plot in Figure 8 further corroborates this finding, as all data points closely align with the fitted line, and no outliers are evident. This uniform distribution of residuals across all runs validates the assumption of normality, justifying the subsequent use of parametric statistical methods such as ANOVA and regression analysis for further evaluation of the mechanical properties of the 3D-printed specimens.

Response Table 4 for Signal-to-Noise (S/N) Ratios and the corresponding Main Effects Plot in Figure 8, the optimal levels of FDM process parameters for enhancing the Ultimate Tensile Strength (UTS) of PLA components were determined using the Taguchi method, employing the "larger is better" quality criterion. The infill percentage had the most significant effect on UTS, with the highest S/N ratio observed at Level 3 (65%), resulting in a delta value of 1.37 dB and ranking first among the studied parameters. This indicates that a higher infill percentage considerably improves mechanical strength by reducing internal voids and enhancing inter-layer bonding, as confirmed by Goh *et al.* [31] and Khosravani & Reinicke [26]. The second most influential factor was print speed, where Level 1 (30 mm/s) exhibited the optimal response with a delta of 0.37 dB. Slower print speed promotes better layer adhesion and reduces the likelihood of void formation, thereby contributing to improved tensile strength. The infill pattern ranked third, showing moderate impact with a delta of 0.31 dB, whereas the extrusion temperature had the least influence on UTS, reflected by its lowest delta value of 0.11 dB. This suggests that the tested temperature range had minimal impact on strength properties, affirming the thermal stability of PLA within these limits.

The main effects plot further support these findings. The infill percentage displayed a steep upward trend, reaffirming its dominant influence on UTS. In contrast, print speed demonstrated a descending pattern, indicating that lower speeds are beneficial for mechanical performance. The effects of infill pattern and extrusion temperature were relatively minimal, aligning with their lower delta values in the response table. Taken together, the optimal combination of parameters for maximizing UTS is identified as: infill pattern at Level 2, infill percentage at Level 3 (65%), print speed at Level 1 (30 mm/s), and extrusion temperature at Level 3 (220°C). This configuration enhances interlayer cohesion, minimizes structural defects, and significantly improves tensile performance, consistent with recent research.

Based on the Analysis of Variance (ANOVA) results and the Model Summary for the Ultimate Tensile Strength (UTS) of FDM 3D-printed PLA specimens, the statistical significance and relative contributions of each process parameter can be clearly interpreted from Table 5. The ANOVA was performed at a 95% confidence level to determine the effect of key printing parameters, namely infill pattern, infill percentage, print speed, and extrusion temperature, on UTS. A p-value threshold of 0.05 was used to establish statistical significance, where parameters with p-values less than 0.05 were considered to have a significant influence on UTS.

Table 4. Response for signal-to-noise ratios

Level	Infill pattern	Infill percentage	Print speed (mm/sec)	Extrusion temp (°C)
1	29.14	28.58	29.35	29.17
2	29.37	29.05	29.24	29.15
3	29.06	29.94	28.98	29.25
Delta	0.31	1.37	0.37	0.11
Rank	3	1	2	4

Table 5. ANOVA for ultimate tensile strength

Source	DF	Adj SS	Adj MS	F-Value	P-Value
Regression	4	33.6863	8.4216	11.31	0.019
Infill pattern	1	0.0600	0.0600	0.08	0.791
Infill percentage	1	31.2360	31.2360	41.95	**0.003***
Print speed (mm/sec)	1	2.2940	2.2940	3.08	0.154
Extrusion temp (°C)	1	0.0963	0.0963	0.13	0.737
Error	4	2.9787	0.7447		
Total	8	36.6650			

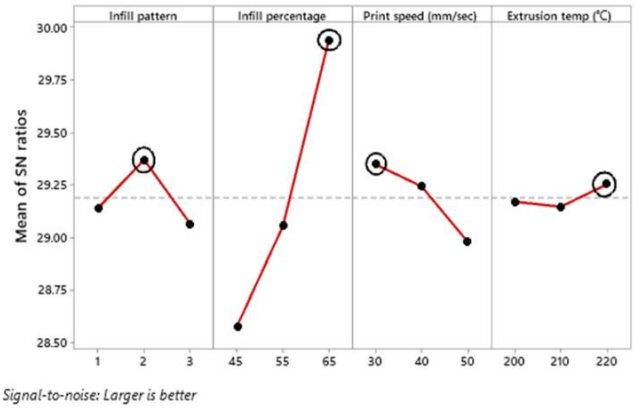

Figure 8. Main effects plot for SN ratios

Among the tested variables, infill percentage was the only statistically significant factor ($p = 0.003$), indicating a strong impact on tensile strength. This aligns with prior studies, which highlight that higher infill percentages reduce internal voids, thereby improving interlayer bonding and mechanical performance [57, 58]. In contrast, infill pattern ($p = 0.791$), print speed ($p = 0.154$), and extrusion temperature ($p = 0.737$) were not statistically significant in this case, suggesting their influence on UTS is comparatively minor within the tested range. These findings emphasize that while infill structure and speed may contribute to mechanical behavior, their effects are overshadowed by infill density when it comes to tensile performance under the given experimental conditions.

The regression model itself was statistically significant ($p = 0.019$), validating the overall model's capability to predict UTS outcomes. The R-squared (R^2) value of 91.88% indicates that a high proportion of the variability in UTS can be explained by the model. The adjusted R^2 value of 83.75% accounts for the number of predictors in the model, reflecting a strong model fit without overfitting. However, the predicted R^2 value of 68.00%, though lower, still reflects a reasonably good predictive performance, suggesting the model generalizes adequately to unseen data. The regression Equation (2) used to predict the model is:

$$\begin{aligned}\text{Ultimate tensile strength (MPa)} &= 16.34 - 0.100\ \text{Infill pattern} \\ &+ 0.2282\ \text{Infill percentage} \\ &- 0.0618\ \text{Print speed (mm/sec)} \\ &+ 0.0127\ \text{Extrusion temp (°C)} \end{aligned} \quad (2)$$

The comparison between the predicted and experimental values of Ultimate Tensile Strength (UTS) is depicted in Figure 9, revealing the performance of the regression model developed through quadratic regression analysis. The plot illustrates the variation in UTS across nine experimental runs, where the blue curve represents the actual experimental results and the orange curve denotes the predicted values from the model. This comparison serves to validate the predictive reliability of the model developed during optimization of FDM printing parameters.

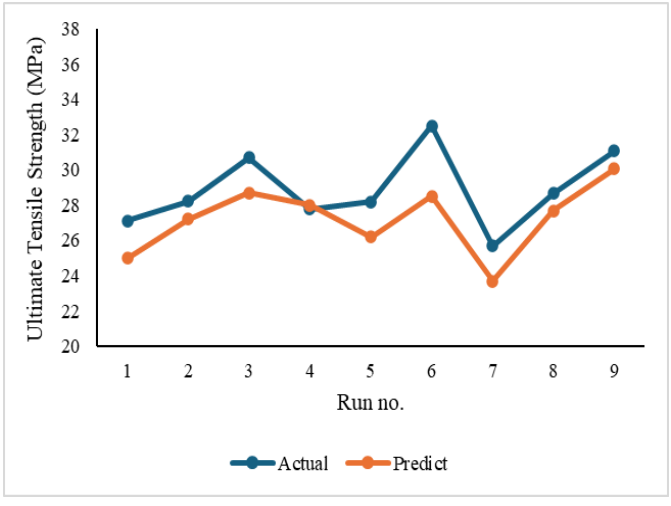

Figure 9. Comparison of predictive value with experimental results for UTS

From the trend observed in Figure 9, the predicted values do not perfectly match the actual results in all runs, but they generally follow a similar pattern. This is consistent with the R-squared (R^2) value of 91.88% reported earlier, indicating a strong correlation between predicted and observed values. However, the difference between the actual and predicted curves suggests that certain nonlinearities or interactions might exist that were not fully captured by the model, as reflected in the lower predicted R^2 value of 68.00%. Despite this, the predicted values fall within an acceptable error margin and are deemed statistically reliable, particularly given that they lie within the 95% confidence interval bounds established for the model.

The model's robustness is further supported by earlier references that emphasize the utility of regression models in evaluating FDM performance parameters [56, 57]. Moreover, this finding agrees with recent literature demonstrating that although statistical models may show small prediction errors, they are still highly useful for guiding process optimization in additive manufacturing [58, 59].

Contour plots are an effective tool for visualizing how two continuous parameters influence a response variable while keeping categorical variables constant. This approach is widely used in manufacturing and materials science to understand the impact of process settings on material performance. In the given Figure 10, three contour plots

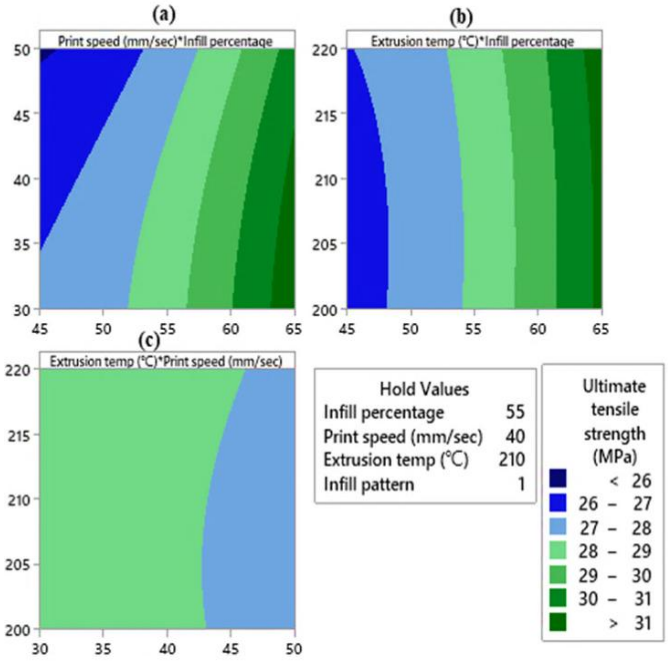

Figure 10. Contour plots show the influence of key 3D printing parameters on ultimate tensile strength (UTS), (a) effect of print speed and infill percentage, (b) effect of extrusion temperature and infill percentage, and (c) effect of extrusion temperature and print speed

depict how combinations of print speed, infill percentage, and extrusion temperature affect the ultimate tensile strength (UTS) of 3D-printed PLA. UTS values increase from blue (< 26 MPa) to green (> 31 MPa). The top-left plot shows that increasing infill percentage and reducing print speed enhance UTS due to improved interlayer bonding. The top-right plot reveals that higher extrusion temperatures and infill percentages lead to better mechanical strength, likely from enhanced layer fusion. The bottom-left plot indicates that elevated temperatures combined with slower speeds also improve UTS, though less significantly. These trends reinforce existing research highlighting extrusion temperature and infill density as key factors in optimizing FDM-printed part strength [48].

4. CONCLUSIONS

This study systematically examined the effects of infill patterns, infill densities, print speed, and extrusion temperature on the ultimate tensile strength (UTS) of FDM-fabricated PLA components. The results demonstrated that infill percentage was the most statistically significant factor influencing UTS, as confirmed by ANOVA ($p = 0.003$), while other parameters, such as infill pattern, print speed, and extrusion temperature, exhibited minimal influence within the tested range. The mechanical properties of PLA samples varied significantly across processing conditions, with UTS ranging from 19.04 MPa to 33.88 MPa. The normal probability plots confirmed the normality of the data without the presence of outliers, thereby validating the statistical analysis.

Among the patterns evaluated, the Quarter Cubic infill at 65% density achieved mechanical performance comparable to fully solid specimens, offering a favorable balance between material efficiency and strength. This finding underscores the potential of infill optimization as a practical strategy for reducing material usage without compromising structural integrity.

Regression analysis yielded a high R^2 value (91.88%), validating the predictive capability of the model. The observed and predicted UTS values were in good agreement, with errors within acceptable limits. Additionally, the normal probability plots and residual analyses confirmed the reliability of the experimental data.

In conclusion, the study provides valuable insights for optimizing FDM process parameters to achieve high-performance PLA components tailored for lightweight and load-bearing applications. Future research should explore fatigue behavior, temperature-dependent performance, and composite-enhanced PLA filaments to further expand the application scope of FDM in engineering and industrial domains.

ACKNOWLEDGMENTS

The authors extend their appreciation to the Ministry of Higher Education, Malaysia, for funding this study under the Fundamental Research Grant Scheme (FRGS) with grant number FRGS/1/2019/TK03/UniMAP/02/3.

CONFLICTS OF INTEREST

The authors have no conflicts of interest to disclose.

REFERENCES

[1] T. D. Ngo, A. Kashani, G. Imbalzano, K. T. Nguyen, and D. Hui, "Additive manufacturing (3D printing): A review of materials, methods, applications and challenges," *Composites Part B: Engineering*, vol. 143, pp. 172–196, 2018.

[2] G. Vashishtha *et al.*, "Shaping the future: latest developments in 3D printing stimuli-responsive soft polymers," *The International Journal of Advanced Manufacturing Technology*, vol. 136, no. 10, pp. 4215–4237, 2025.

[3] "Standard terminology for additive manufacturing technologies," *ASTM International F2792-12a*, vol. 46, pp. 10 918– 10 928, 2012.

[4] A. Gebhardt and J.-S. Hotter, "Additive manufacturing: 3D printing for prototyping and manufacturing." Carl Hanser Verlag GmbH Co KG, 2016.

[5] M. Attaran, "The rise of 3-D printing: The advantages of additive manufacturing over traditional manufacturing," *Business Horizons*, vol. 60, no. 5, pp. 677–688, 2017.

[6] N. Shahrubudin, T. C. Lee, and R. Ramlan, "An overview on 3D printing technology: Technological, materials, and applications," *Procedia Manufacturing*, vol. 35, pp. 1286–1296, 2019.

[7] B. Rankouhi, S. Javadpour, F. Delfanian, and T. Letcher, "Failure analysis and mechanical characterization of 3D printed abs with respect to layer thickness and orientation," *Journal of Failure Analysis and Prevention*, vol. 16, no. 3, pp. 467–481, 2016.

[8] S. Khan, K. Joshi, and S. Deshmukh, "A comprehensive review on effect of printing parameters on mechanical properties of FDM printed parts," *Materials Today: Proceedings*, vol. 50, pp. 2119–2127, 2022.

[9] F. P. Melchels, M. A. Domingos, T. J. Klein, J. Malda, P. J. Bartolo, and D. W. Hutmacher, "Additive manufacturing of tissues and organs," *Progress in Polymer Science*, vol. 37, no. 8, pp. 1079–1104, 2012.

[10] Z. Yin, K. M. Clark, and T. R. Ray, "Emerging additive manufacturing methods for wearable sensors: Opportunities to expand access to personalized health monitoring," *Advanced Sensor Research*, vol. 3, no. 3, p. 202470010, 2024.

[11] A. K. Sood, R. K. Ohdar, and S. S. Mahapatra, "Parametric appraisal of mechanical property of fused deposition modelling processed parts," *Materials & Design*, vol. 31, no. 1, pp. 287–295, 2010.

[12] A. R. Torrado and D. A. Roberson, "Failure analysis and anisotropy evaluation of 3D-printed tensile test specimens of different geometries and print raster patterns," *Journal of Failure Analysis and Prevention*, vol. 16, no. 1, pp. 154–164, 2016.

[13] M. Domingo-Espin, J. M. Puigoriol-Forcada, A.-A. Garcia-Granada, J. Lluma, S. Borros, and G. Reyes,

"Mechanical property characterization and simulation of fused deposition modeling polycarbonate parts," *Materials & Design*, vol. 83, pp. 670–677, 2015.

[14] P. Chansamai, T. Seangpong, and V. Uthaisangsuk, "Effect of raster and layer characteristics on tensile behavior and failure of FFF printed pla samples by representative volume element model," *Proceedings of the Institution of Mechanical Engineers, Part B: Journal of Engineering Manufacture*, vol. 238, no. 10, pp. 1463–1473, 2024.

[15] M. A. Islam, N. S. Kamarrudin, M. F. Ijaz, T. Furuki, K. S. Basaruddin, and R. Daud, "Soft material drilling: A thermo-mechanical analysis of polyurethane foam for biomimetic bone scaffolds and optimization of process parameters using taguchi method," *Heliyon*, vol. 10, no. 17, 2024.

[16] K. S. Patel, D. B. Shah, S. J. Joshi, F. K. Aldawood, and M. Kchaou, "Effect of process parameters on the mechanical performance of fdm printed carbon fiber reinforced petg," *Journal of Materials Research and Technology*, vol. 30, pp. 8006–8018, 2024.

[17] J. M. Chacon, M. A. Caminero, E. Garcıa-Plaza, and P. J. Nunez, "Additive manufacturing of pla structures using fused deposition modelling: Effect of process parameters on mechanical properties and their optimal selection," *Materials & Design*, vol. 124, pp. 143–157, 2017.

[18] A. Alafaghani, A. Qattawi, B. Alrawi, and A. Guzman, "Experimental optimization of fused deposition modelling processing parameters: a design-for-manufacturing approach," *Procedia Manufacturing*, vol. 10, pp. 791–803, 2017.

[19] R. Tino *et al.*, "Covid-19 and the role of 3D printing in medicine," *3D Printing in Medicine*, vol. 6, no. 1, p. 11, 2020.

[20] S. Ishack and S. R. Lipner, "Use of 3D printing to support Covid-19 medical supply shortages: a review," *Journal of 3D printing in Medicine*, vol. 5, no. 2, pp. 83–95, 2021.

[21] J. L. Amaya-Rivas *et al.*, "Future trends of additive manufacturing in medical applications: An overview," *Heliyon*, vol. 10, no. 5, 2024.

[22] M. Abas, T. Habib, S. Noor, B. Salah, and D. Zimon, "Parametric investigation and optimization to study the effect of process parameters on the dimensional deviation of fused deposition modeling of 3D printed parts," *Polymers*, vol. 14, no. 17, p. 3667, 2022.

[23] M. R. de Campos, A. L. Botelho, and A. C. dos Reis, "Antimicrobial incorporation on 3D-printed polymers used as potential dental materials and biomaterials: a systematic review of the state of the art," *Polymer Bulletin*, vol. 80, no. 7, pp. 7313–7340, 2023.

[24] J. M. Cañero-Nieto, R. J. Campo-Campo, I. Díaz-Bolaño, E. A. Ariza-Echeverri, C. E. Deluque-Toro, and J. F. Solano-Martos, "Infill pattern strategy impact on the cross-sectional area at gauge length of material extrusion 3D printed polylactic acid parts," *Journal of Intelligent Manufacturing*, vol. 37, no. 3, pp. 977–998, 2026.

[25] V. S. Jatti *et al.*, "Optimization of tensile strength in 3D printed PLA parts via meta-heuristic approaches: a comparative study," *Frontiers in Materials*, vol. 10, 2024.

[26] M. A. Islam, N. S. B. Kamarrudin, M. F. Ijaz, R. Daud, K. S. Basaruddin, A. N. Abdullah, and H. Takemura, "Supervised machine learning to predict drilling temperature of bone," *Applied Sciences*, vol. 14, no. 17, p. 8001, 2024.

[27] A. S. Karad, P. D. Sonawwanay, M. Naik, and D. Thakur, "Experimental study of effect of infill density on tensile and flexural strength of 3D printed parts," *Journal of Engineering and Applied Science*, vol. 70, no. 1, p. 104, 2023.

[28] M. Waseem *et al.*, "Multi-response optimization of tensile creep behavior of PLA 3D printed parts using categorical response surface methodology," *Polymers*, vol. 12, no. 12, p. 2962, 2020.

[29] N. C. Paxton and M. A. Woodruff, "Measuring contact angles on hydrophilic porous scaffolds by implementing a novel raised platform approach: A technical note," *Polymers for Advanced Technologies*, vol. 33, no. 10, pp. 3759–3765, 2022.

[30] Z. Lv *et al.*, "A MGFE-LDH nanosheet-incorporated smart thermoresponsive hydrogel with controllable growth factor releasing capability for bone regeneration," *Advanced materials*, vol. 35, no. 5, p. 2206545, 2023.

[31] Y. Zhou, J. Chen, X. Liu, and J. Xu, "Three/four-dimensional printed pla nano/microstructures: crystallization principles and practical applications," *International Journal of Molecular Sciences*, vol. 24, no. 18, p. 13691, 2023.

[32] G. Ma, Y. Chen, W. Dong, M. Xu, T. Li, and H. Wang, "Investigation of nuclide migration in complex fractures with filling properties," *Journal of Cleaner Production*, vol. 403, p. 136781, 2023.

[33] M. Tadesse and Y. Liu, "Recent advances in enzyme immobilization: The role of artificial intelligence, novel nanomaterials, and dynamic carrier systems," *Catalysts*, vol. 15, no. 6, p. 571, 2025.

[34] K. Benié, T. Barrière, V. Placet, and A. Cherouat, "Introducing a new optimization parameter based on diffusion, coalescence and crystallization to maximize the tensile properties of additive manufacturing parts," *Additive Manufacturing*, vol. 69, p. 103538, May 2023.

[35] M. A. Cuiffo, J. Snyder, A. M. Elliott, N. Romero, S. Kannan, and G. P. Halada, "Impact of the Fused Deposition (FDM) Printing Process on Polylactic Acid (PLA) Chemistry and Structure," *Applied Sciences*, vol. 7, no. 6, p. 579, 2017.

[36] M. Derise and A. Zulkharnain, "Effect of Infill Pattern and Density on Tensile Properties of 3D Printed Polylactic acid Parts via Fused Deposition Modeling (FDM)," *International Journal of Mechanical & Mechatronics Engineering*, vol. 20, pp. 54–62, 2021.

[37] A. Dadashi and M. Azadi, "Multi-objective numerical optimization of 3D-printed polylactic acid bio-metamaterial based on topology, filling pattern, and infill density via fatigue lifetime and mass," *Plos one*, vol. 18, no. 9, p. e0291021, 2023.

[38] M. Memiş and D. A. Gök, "Development of Fe-reinforced PLA-based composite filament for 3D printing: Process parameters, mechanical and microstructural characterization," *Ain Shams Engineering Journal*, vol. 16, no. 2, p. 103279, 2025.

[39] M. S. Kiran Karthik, H. K. R. Karanam, and S. S. Prabu, "Experimental and Thermal Analysis of Desktop FDM 3D Printers 'Ender 3' and 'CR-10S Pro' Hot Ends," *ECS Transactions*, vol. 107, no. 1, pp. 12851–12862, 2022.

[40] K. S. Boparai, R. Singh, and H. Singh, "Development of rapid tooling using fused deposition modeling: a review," *Rapid Prototyping Journal*, vol. 22, no. 2, pp. 281–299, 2016.

[41] E. B. Hungria, F. G. Di Nisio, F. C. Cano, R. Voltolini, and N. Volpato, "A study about weak intralayer bonding in extrusion-based additive manufacturing due to resumed extrusion during filling," *Polymer Testing*, vol. 140, p. 108595, 2024.

[42] S. R. Rajpurohit and H. K. Dave, "Effect of process parameters on tensile strength of FDM printed PLA part," *Rapid Prototyping Journal*, vol. 24, no. 8, pp. 1317–1324, 2018.

[43] M. A. Islam, N. S. Kamarrudin, M. F. F. Suhaimi, R. Daud, I. Ibrahim, and F. Mat, "Parametric Investigation on Different Bone Densities to avoid Thermal Necrosis during Bone Drilling Process," *Journal of Physics: Conference Series*, vol. 2051, no. 1, p. 012033, 2021.

[44] M. A. Islam, N. S. Kamarrudin, R. Daud, I. Ibrahim, Z. M. Razlan, and M. F. H. Rani, "Drill Bit Design and Its Effect on Temperature Distribution and Osteonecrosis During Implant Site Preparation: An Experimental Approach," *Journal of Physics: Conference Series*, vol. 2643, no. 1, p. 012020, 2023.

[45] R. Agarwal, J. Singh, and V. Gupta, "A data-driven ensemble machine learning approach for predicting the mechanical strength of 3D printed orthopaedic bone screws," *Proceedings of the Institution of Mechanical Engineers, Part E: Journal of Process Mechanical Engineering*, vol. 239, no. 4, pp. 1650–1662, 2025.

[46] Y. Zhao, Y. Chen, and Y. Zhou, "Novel mechanical models of tensile strength and elastic property of FDM AM PLA materials: Experimental and theoretical analyses," *Materials & Design*, vol. 181, p. 108089, 2019.

[47] S. R. Rajpurohit and H. K. Dave, "Effect of process parameters on tensile strength of FDM printed PLA part," *Rapid Prototyping Journal*, vol. 24, no. 8, pp. 1317–1324, 2018.

[48] L. Marşavina *et al.*, "Effect of the manufacturing parameters on the tensile and fracture properties of FDM 3D-printed PLA specimens," *Engineering Fracture Mechanics*, vol. 274, p. 108766, 2022.

[49] M. Tahir and A.-F. Seyam, "Greening fused deposition modeling: A critical review of plant fiber-reinforced PLA-based 3D-printed biocomposites," *Fibers*, vol. 13, no. 5, p. 64, 2025.

[50] A. Garg, A. Bhattacharya, and A. Batish, "Failure investigation of fused deposition modelling parts fabricated at different raster angles under tensile and flexural loading," *Proceedings of the Institution of Mechanical Engineers, Part B: Journal of Engineering Manufacture*, vol. 231, no. 11, pp. 2031–2039, 2017.

[51] A. A. F. Ogaili *et al.*, "The effect of chopped carbon fibers on the mechanical properties and fracture toughness of 3D-printed PLA parts: an experimental and simulation study," *Journal of Composites Science*, vol. 8, no. 7, p. 273, 2024.

[52] A. Hanchate, S. T. Bukkapatnam, K. H. Lee, A. Srivastava, and S. Kumara, "Explainable AI (XAI)-driven vibration sensing scheme for surface quality monitoring in a smart surface grinding process," *Journal of Manufacturing Processes*, vol. 99, pp. 184–194, 2023.

[53] L. Suárez and M. Domínguez, "Sustainability and environmental impact of fused deposition modelling (FDM) technologies," *The International Journal of Advanced Manufacturing Technology*, vol. 106, no. 3–4, pp. 1267–1279, 2020.

[54] O. Tunçel, K. Tüfekci, and Ç. Kahya, "Multi-objective optimization of 3D printing process parameters using gray-based Taguchi for composite PL parts," *Polymer Composites*, vol. 45, no. 14, pp. 12870–12884, 2024.

[55] A. K. Sood, R. K. Ohdar, and S. S. Mahapatra, "Improving dimensional accuracy of Fused Deposition Modelling processed part using grey Taguchi method," *Materials & Design*, vol. 30, no. 10, pp. 4243–4252, 2009.

[56] J. Castro *et al.*, "Density-Based Topology-Optimized 3D-Printed Fixtures for Cyclic Mechanical Testing of Lattice Structures," *Polymers*, vol. 17, no. 18, p. 2468, 2025.

[57] B. Singaravel, T. Niranjan, M. Vasu Babu, and K. Nagarjuna, "Optimization of Fused Deposition Modeling Control Parameters Using Hybrid Taguchi and TOPSIS Method," in *Sustainable Machining and Green Manufacturing*, Wiley, 2024, pp. 289–304.

[58] M. A. B. Syed, Q. Rhaman, H. M. Shahriar, and M. M. A. Khan, "Grey-taguchi approach to optimize fused deposition modeling process in terms of mechanical properties and dimensional accuracy," *Journal of Engineering Research, Innovation and Education*, vol. 4, no. 1, pp. 38–52, 2022.

[59] X. Liu, M. Zhang, S. Li, L. Si, J. Peng, and Y. Hu, "Mechanical property parametric appraisal of fused deposition modeling parts based on the gray taguchi method," *The International Journal of Advanced Manufacturing Technology*, vol. 89, no. 5, pp. 2387–2397, 2017.